

**MODELING WELLBORE PRESSURE WITH APPLICATION TO
MULTI-STAGE, ACID-STIMULATION TREATMENT**

A Thesis

by

EFEJERA A. EJOFODOMI

Submitted to the Office of Graduate Studies of
Texas A&M University
in partial fulfillment of the requirements for the degree of

MASTER OF SCIENCE

May 2006

Major Subject: Petroleum Engineering

**MODELING WELLBORE PRESSURE WITH APPLICATION TO
MULTI-STAGE, ACID-STIMULATION TREATMENT**

A Thesis

by

EFEJERA A. EJOFODOMI

Submitted to the Office of Graduate Studies of
Texas A&M University
in partial fulfillment of the requirements for the degree of

MASTER OF SCIENCE

Approved by:

Chair of Committee,
Committee Members,

Head of Department,

Ding Zhu
Dan A. Hill
Taher Schobeiri
Steve Holditch

May 2006

Major Subject: Petroleum Engineering

ABSTRACT

Modeling Wellbore Pressure with Application to Multi-stage, Acid-stimulation

Treatment. (May 2006)

Efejera A. Ejofodomi, B.S., University of Lagos, Nigeria

Chair of Advisory Committee: Dr. Ding Zhu

Estimation of bottomhole pressure during a matrix-acidizing treatment provides the information needed to accurately determine the evolution of skin factor during and after the treatment. It could be a very complicated process, especially when compressible fluids, such as foams, are involved. Existing models for estimating bottomhole pressure during a matrix-acidizing treatment ignore the volume reduction of compressible fluids and its effect on the bottomhole pressure.

This research developed a model that uses a unique solution to the mechanical energy balance equation, to calculate the bottomhole pressure from known surface measurements during foamed acid stimulation. The model was used to evaluate two stimulation treatments. Field examples are presented which illustrate the application of the model to optimize stimulation treatments.

Properly accounting for the flow behavior and tracking the injected volume of the foam diverter used during the treatment resulted in more reliable and accurate bottomhole pressure profile.

DEDICATION

This thesis is dedicated to the Almighty God, for the love, wisdom, and protection he has granted me up until this moment in my life. It is dedicated to my loving, caring, and supportive family, for all their prayers and support needed to complete this work.

To the one and only true love of my life, Onome, who came into my life as a blessing and filled up the emptiness in me.

Finally I will to dedicate this work to my long and dearest friend, Imonite, whom I didn't see before he passed away.

ACKNOWLEDGEMENTS

The author wishes to express his sincere gratitude and appreciation to the following people who greatly contributed in no small measure to this work: Dr. Ding Zhu, Assistant Professor of Petroleum Engineering, who served as the chair of my graduate committee. Her dedication, support, and enthusiasm guided me to the completion of this work. It has being a real pleasure and privilege to work under such supervision.

Drs. Dan Hill and Taher Schobeiri, for serving as members of my graduate committee.

Additionally, the successful completion of my thesis would not have been possible without the blessing and support of my dear friend Kola Ayeni.

TABLE OF CONTENTS

	Page
ABSTRACT	iii
DEDICATION	iv
ACKNOWLEDGEMENTS	v
TABLE OF CONTENTS	vi
LIST OF TABLES	ix
LIST OF FIGURES.....	x
CHAPTER I INTRODUCTION	1
1.1 Matrix Acidizing	1
1.2 Foam Diversion	2
1.3 Pressure-Drop Calculations	3
1.4 Rheological Behavior of Fluids.....	4
1.5 Objectives and Procedures	6
CHAPTER II LITERATURE REVIEW	8
2.1 Introduction	8
2.2 Pressure-Drop Calculations.....	8
2.3 Characteristics of Foams	11
2.3.1 Foam Generation	11
2.3.2 Foam Quality	12
2.3.3 Foam Stability	12
2.3.4 Foam Compressibility	12
2.3.5 Rheological Equations.....	14
2.4 Fluid-Length Tracking	16
CHAPTER III PRESSURE-DROP MODEL DEVELOPMENT	18
3.1 Overview	18
3.2 Analytical Model Development	18
3.2.1 Equation of State	19
3.2.2 Rheological Model	20

	Page
3.2.3 Pressure-Drop Model	22
3.3 Friction Factor	25
3.4 Fluid-Length Tracking	26
CHAPTER IV SKIN FACTOR EVOLUTION IN MATRIX ACIDIZING	33
4.1 Overview	33
4.2 Matrix-acidizing Evaluation.....	33
CHAPTER V DEVELOPMENT OF PROGRAM FOR BOTTOMHOLE PRESSURE CALCULATION.....	37
5.1 Program Outline	37
5.2 Model Validation.....	38
CHAPTER VI FIELD APPLICATION EXAMPLES	42
6.1 Matrix-acidizing Stimulation Examples.....	42
6.2 Tracking Injected-Fluid Length	47
CHAPTER VII CONCLUSIONS AND RECOMMENDATIONS.....	49
7.1 Conclusions	49
7.2 Recommendations	49
NOMENCLATURE.....	50
REFERENCES.....	54
APPENDIX A	60
VITA.....	70

LIST OF TABLES

TABLE	Page
1.1 SHEAR STRESS-SHEAR STRAIN RELATIONSHIP FOR MAJOR FLUID CLASSIFICATION	4
5.1 INPUT DATA ¹⁴ FOR CASE 2	39
5.2 PREDICTED VS ACTUAL BHP (DATA FROM LORD ¹⁴)	39
6.1 FLUID TREATMENT SCHEDULE FOR FIELD EXAMPLE	41
6.2 FLUID TREATMENT SCHEDULE FOR ARBITRARY EXAMPLE	47

LIST OF FIGURES

FIGURE		Page
1.1	Rheological curves for all fluids show that only Herschel-Bulkley and Bingham plastic fluid exhibits a yield stress necessary to initiate movement	5
5.1	Flow chart for estimating the bottomhole pressure (BHP) for stimulating fluids including foam	37
5.2	Effect of proppant on predicted BHP	40
6.1	Field treatment history	42
6.2	Cut-out section of the field treatment used for analysis.....	44
6.3	Bottomhole pressure and injection rate history for field example	45
6.4	Calculated skin factor history.....	46
6.5	Effect of foam volume reduction on the estimated BHP.....	48

CHAPTER I

INTRODUCTION

1.1 Matrix Acidizing

Matrix acidizing is a form of well stimulation techniques that involves the injection of acid into the formation to remove near wellbore damage, thereby improving the overall productivity. One major advantage of matrix acidizing over other stimulation techniques is its relatively low cost. This low cost has retarded the overall technological development of the process compared to hydraulic or acid fracturing.

In matrix acidizing, the acid is generally injected at pressures below the breakdown pressure of the formation so that fractures will not be created. This is the major difference between matrix acidizing and acid fracturing, where in the latter, acid is injected above the formation breakdown pressure to create fractures. For near-wellbore damage matrix acidizing can greatly enhance the productivity of a well, and generally as a rule of thumb, is applied only in situations where a well has a large skin effect that cannot be attributed to mechanical, operation or surface problems.

Real-time monitoring is an effective way of optimizing matrix-acidizing treatments¹⁻⁵ from injected flowrate and bottomhole pressure, BHP through the evaluation of the skin factor evolution. The skin factor is obtained using the measured BHP and flowrate.

This thesis follows the style of *SPE Production & Facilities*.

In general, bottomhole pressure is not measured during acid treatments because of corrosion on the pressure gauges by the acid; it is estimated from the measured surface pressure.

Proper acid placement is a critical factor for a successful matrix-acidizing treatment. Complete damage removal is not guaranteed even in a homogenous formation; therefore for an optimal treatment, acid placement and distribution should be planned and executed efficiently.⁶

1.2 Foam Diversion

Diversion is a common method used for effective acid placement. Methods of diversion include ball sealers, mechanical zone isolation, particulate diverting agents, and foams. The diverting method of interest in this research is foam diversion.

Foams are generally created by mixing a discontinuous gaseous phase (normally nitrogen or carbon dioxide) with a continuous liquid phase—either water (stable foam) or an aqueous polymer solution containing 1 to 2% by volume a foaming agent for stability. These are called two-phase or neat foams (no solid phase). For most hydraulic fracturing treatments, three-phase foams are normally formed by the addition of a solid phase (proppant). The manner in which the individual phases are distributed in the wellbore greatly affects the slippage between these phases and the pressure drop. Slippage has an effect on the enthalpy and in-situ foam quality (volume fraction of gas at actual flow condition), thereby resulting in the accumulation of liquid and a corresponding decrease in quality.

The major advantages of foam include high viscosity (greater than both liquid and gaseous phases), low liquid content, good cuttings-transport capacity, and instability on contact with oil. These advantages have propelled the use of foams in a number of petroleum-industrial applications: as a displacing agent in porous media, underbalanced drilling and wellbore circulating fluid; and as a stimulating fluid during acidizing and hydraulic fracturing treatments.

Foam has low mobility in rock which enables the effective diversion of acid during field applications. This mobility reduction can be represented as either a reduction in permeability ⁶, or an increase in viscosity; in reality, it is a combination of both.⁷ On contact with oil, foam breaks down or collapse, which enables it to block out watered-zones in field applications. Like viscosified fluids, foam increases the resistance to flow into a given interval through mobility reduction and imparts a skin factor which is constant for a batch treatment, but increases for continuous foam injection.

1.3 Pressure-Drop Calculations

The pressure drop experienced during matrix acidizing is strongly dependent on the type of injected fluid, flowrate, and on the reservoir pressure and temperature. Inaccurate prediction of bottomhole pressure in acid-treatment monitoring can lead to the misunderstanding of the matrix-acidizing process that sometimes results in higher treatment cost than necessary or even additional damage to the formation.

Due to the compressible nature of foam, its rheological properties change as it travels down the wellbore; therefore to accurately predict the pressure drop of foam, an

iterative solution to has to be employed. Accurately predicting the pressure drop along the well requires an understanding of the rheological behavior of foam, especially under the bottomhole conditions of high pressure and temperature.

1.4 Rheological Behavior of Fluids

Rheology is the study of the deformation and flow of matter, or simply put, the relationship between the applied stress and the resulting motion of the fluid. Fluids are generally classified under one of four groups as shown in **Table 1.1**.

TABLE 1.1—SHEAR STRESS-SHEAR STRAIN RELATIONSHIP FOR MAJOR FLUID CLASSIFICATION.	
Model	Mathematical equation
Newtonian fluids	$\tau = \mu\gamma$
Bingham plastic fluids	$\tau = \tau_{yp} + \mu\gamma$
Power law fluids	$\tau = k\gamma^n$
Herschel-Bulkley (HB) fluids	$\tau = \tau_{yp} + k\gamma^n$

Newtonian is the simplest of all fluids, with a constant, shear-independent viscosity. As seen from **Fig. 1.1**, the rheological curve is a straight line, with a constant-positive slope through the origin. All fluids that deviate from this behavior are called non-Newtonian fluids.

Bingham plastic fluids are analogous to the Newtonian fluid, but require a positive shear stress, which is the intercept of the curve to initiate flow, and the obtained slope is called the *plastic viscosity*.

Power law fluids exhibit no yield stress and the slope changes with the shear rate; if the slope decreases, the fluid is called *pseudoplastic* fluid; if it increases, it is called a *dilatant* fluid.

Herschel-Bulkley fluids are also called *yield pseudoplastic* fluids because they behave like the pseudoplastic fluid but also require a positive yield stress to initiate flow.

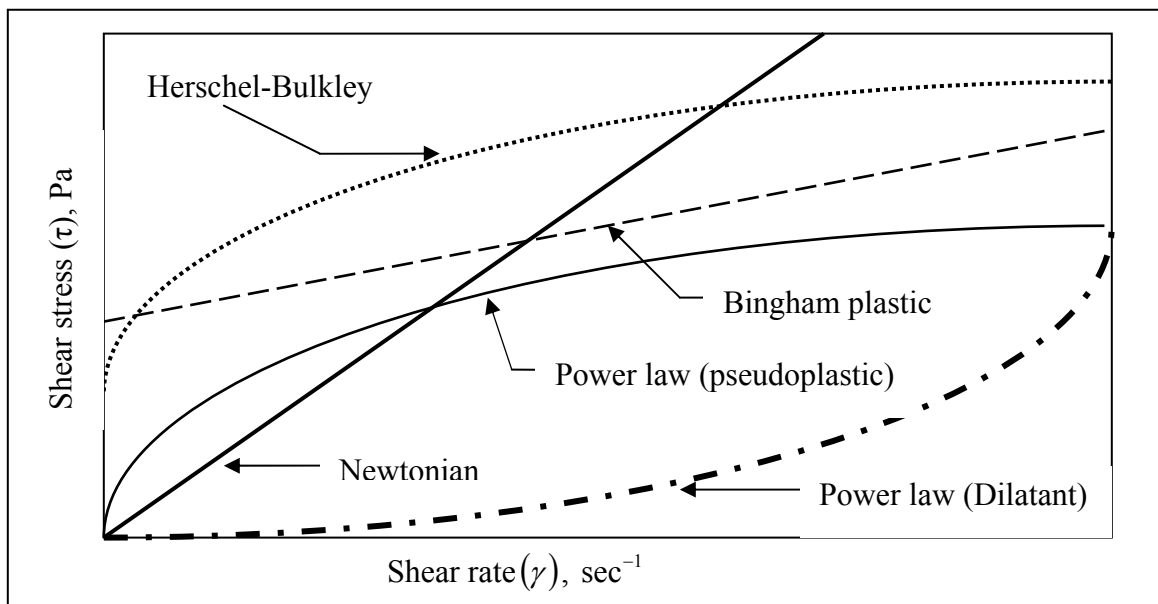


Fig. 1.1—Rheological curves for all fluids show that only Herschel-Bulkley and Bingham plastic fluids exhibit a yield stress necessary to initiate movement.

The study of foam rheology has been the subject of numerous investigations over the last three decades. These can be divided into three approaches:

- Development of rheological equations based on experimental studies using rheometers.

- Rheological measurement in conditions simulating petroleum industrial situations.
- Description of foam rheology through theoretical studies based on microscopic models.

A general insight on the numerous studies carried out on the rheology of foam can be found in literature.^{8, 9} The first impression is the great disagreement between the different results and the frequent nonreproducibility of the measurements, which shows that foam is a complicated fluid.

1.5 Objectives and Procedures

This research accomplishes four goals:

1. Development of a new iterative-computational model for calculating bottomhole pressure during a matrix-acidizing treatment, including tracking the length of individual fluid column including foam in the wellbore
2. Development of a user-friendly program to provide pretreatment analysis to evaluate the skin factor and treatment afterwards (posttreatment).
3. Validate the model with previous models and field data.
4. Discuss the importance of bottomhole pressure prediction during matrix acidizing through field cases.

Establishing the appropriate rheological model allowed the frictional factor to be determined at any part of the wellbore. For this research, the Reindenbach *et al.*¹⁰ yield pseudoplastic rheological model was applied.

The real gas law was used to develop an equation of state (EOS) that incorporates the no-slip liquid holdup and neglects the presence of solids (proppants). A unique solution to the mechanical energy balance equation was then obtained and a user-friendly program was developed to estimate the bottomhole pressure during the flow of foam.

Though several foam pressure-prediction models can be found in literature, the model in this project incorporates something new namely; the tracking of the injected length of foam. The developed program estimates pressure losses not only for foam flow, but also for all other stimulating fluids used during a matrix-acidizing treatment, thereby making this new model comprehensive.

CHAPTER II

LITERATURE REVIEW

2.1 Introduction

A lot of researches conducted on the flow of foam can be found in literature, and they can generally be categorized into two groups:

- Foam rheometry using capillaries or rotational viscometers.
- Foam flow in pipes.

This research deals with the flow of foam in pipes; and it is discussed in detail.

2.2 Pressure-Drop Calculations

To estimate bottomhole treating pressure during the injection of foam, the pressure variation along the wellbore must be considered. Some methods¹¹⁻¹³ calculate frictional and hydrostatic pressure losses, but unlike incompressible fluids, totaling the overall pressure drop for foams (compressible fluid) by adding frictional and hydrostatic pressures components would give erroneous results, because they are both interdependent through the pressure-dependent density.¹⁴ The pertinent question still remains: how do we predict the bottomhole pressure during foam treatment and combine the different controllable variables to achieve an efficient and effective treatment?

Techniques which use iterative methods (either length or pressure steps) for transverse wellbore calculations provide the best means of accounting for this interdependence of the dynamic frictional and hydrostatic pressures.¹⁴⁻¹⁷

From a modified Buckingham-Reiner equation, Krug and Mitchell¹¹ developed a numerical method to analyze tubing and annulus flow of foam as a drilling fluid. By averaging foam properties (density, plastic viscosity, and yield stress), they calculated incremental pipe lengths from fixed pressure steps. But the Buckingham-Reiner equation is for laminar pipe flow obtained from a particular rheological model. Therefore, this particular model would not be valid for different rheological models or for turbulent flow.

Beyer *et al.*¹² developed a finite-difference (iterative) method with fixed 5-psi (34.5-KPa) pressure steps, but unlike Krug and Mitchell, they used a semiempirical flow equation formulated from experimental data to describe the steady-state flow of foam in circular pipes. Their model accounted for slippage at the pipe walls. They suggest that including liquid holdup effects during foam circulation in large diameter wells would improve the accuracy of the results.

Assuming the Bingham plastic rheological model, Blauer *et al.*¹³ developed an equivalent or effective Newtonian viscosity for predicting frictional pressures during foam flow in pipes. They used a mass-balance equation and the real gas law to determine the volume changes of the gaseous phase and its properties. The compressibility of foam was neglected in their EOS.

Blauer and Kohlhaas¹⁵ divided the wellbore length into segments which enabled them to monitor the changes in foam viscosity, velocity, quality, density and pressure as it moved down the wellbore. They applied the method proposed by Blauer *et al.*¹³ in calculating an effective viscosity, then calculated the frictional pressure loss and

hydrostatic head for each segment from this effective viscosity. Negligible gas-phase density was also assumed in their calculations.

Lord¹⁴ stressed that the actual density of foam should be used in pressure-loss calculations. He developed a unique EOS which he used to solve the mechanical energy balance equation for both static and dynamic foam flow—by assuming a constant friction factor and no phase holdup.

Preserving the same assumptions as Lord, Sporker *et al.*¹⁷ proposed an improved solution to the mechanical energy equation that used a special form of the virial equation (truncated after the second term to describe the behavior of gas) rather than the engineering gas law used by Lord. Valko and Economides¹⁷ introduced the volume-equalized power law model for polymer foams. They applied their model successfully to large-scale horizontal pipes with different diameters.

For flowing foam up a vertical cylindrical annulus, Okpobiri and Ikoku¹⁹ estimated the pressure drop by correlating the frictional factor by the expression $f = \frac{24}{N_{RE}}$; the Reynolds number, N_{RE} , was based on foam velocity, density and an effective viscosity, which was not clearly defined.

In an attempt to select the best hydraulic model for foam flow, Nakagawa *et al.*²⁰ compared the predictive capability of four different commercial simulators with measured field data and observed significant differences between them. Similarly, Ozbayoglu *et al.*²¹ compared the performance of six different hydraulic models for predicting pressure losses in pipe flow with experimental results and found a deviation

of 2 to 250%. They concluded that no “best” model for predicting foam flow in pipes under all circumstances exists; therefore, the specific application of foam should influence the development of a pressure-drop model.

2.3 Characteristics of Foam

Foams are characterized in various different ways. For accurate pressure calculations, its properties or characteristics have to be understood. The next few sections will go through the important characteristics of foam and their relationship with each other.

2.3.1 Foam Generation

Foam can be created either in-situ by injecting surfactant solution and gas or by circulating the liquid portion first and then injecting the gas into the solution. As energized fluids, N₂ was initially used as the internal or discontinuous phase, but the introduction of CO₂ enabled the industry to achieve deeper well stimulation. N₂ internal-phase foams have lower hydrostatic pressure compared to CO₂ foams, resulting in a higher surface treating pressure to achieve the same bottomhole pressure—provided the frictional pressure drop does not surpass the hydrostatic pressure. By varying the gas and liquid flowrates, different qualities of foams can be attained.

2.3.2 Foam Quality

Foams are generally described by their quality. Krug and Mitchell¹¹ defined the quality of foam as the percentage volume of gas contained within the foam at in-situ condition. This is generally recognized in the petroleum industry and is expressed mathematically as:

$$\Gamma = \left(\frac{V_g}{V_g + V_l} \right) \times 100\% . \quad (2.1)$$

Where Γ is the foam quality, V_g is the volume of the gas phase which is a function of pressure and temperature, and V_l is the volume of the liquid phase. This quality is not constant, but changes down the wellbore as pressure changes. The quality of foam has a limit between 0 and 100%. With the presence of proppant, the corresponding proppant volume is added to the denominator of Eq. 2.1.

2.3.3 Foam Stability

The tendency of the bubbles in foam to resist breakdown is referred to as foam stability. Generally, stabilizers are added during the generation of foam to prevent its breakdown during operation.

2.3.4 Foam Compressibility

Foam basically consists of compressible gas; thus, it is greatly influenced by pressure changes. Gas viscosity changes as a result of pressure changes are small when compared with density changes. Accurately correcting for both acceleration losses and

density changes, allows gases to be represented by Newtonian-fluid laminar and turbulent flow expressions. Thus foams can be represented as a homogeneous fluid with both variable density and viscosity; therefore making it probably the only known compressible non-Newtonian fluid.¹⁴

The EOS proposed by Ross²² had little engineering application due to the difficulty in evaluating parameters in the equation. David and Marsden²³ proposed the use of both a compressibility factor and foam quality in their EOS. But Pressure/volume dependence of both parameters has to be established before applying their EOS.

Heuy and Bryant²⁴ developed an EOS for bubbly two-phase flow, and extended it for foams using the ideal gas law to describe the gaseous (compressible) phase. It could be useful if both its complicated form and the ideal gas-phase behavior assumption can be accepted.

Lord¹⁴ developed a complicated EOS from the basic approach of Heuy and Bryant²⁴ with the possible presence of solids (proppants). He used the engineering or real gas law to represent the gaseous phase. In their analytical-pressure model, Valko and Economides¹⁸ proposed the “specific volume expansion ration”. They accounted for the compressibility of the gaseous phase through a viriel like EOS (truncated after the first term).

2.3.5 Rheological Equations

Developing an analytical solution that accurately predicts foam pressure requires an explicit expression that accurately describes the rheology of foams. Several rheological equations have been proposed from experimental results that describe foam as a non-Newtonian fluid. David and Marsden,²³ Raza and Marsden,²⁵ Patton *et al.*,²⁶ Sanghani and Ikoku,²⁷ Thondavadi and Lemlich,²⁸ and Enzendorfer *et al.*²⁹ described the rheological properties of foam using the Pseudoplastic power-law model. Khan *et al.*³⁰ observed foam in steady state to behave as a Bingham plastic fluid. Reindenbach *et al.*,¹⁰ Calvert and Nezhati,³¹ and Burley and Shakarin,³² all treated foam as a Herschel-Bulkley fluid in describing their respective rheological experiments.

Despite the disagreement by the authors in describing the rheological behavior of foams, they all agree that the apparent viscosity of foam for a given shear rate increases with foam quality. Valko and Economides¹⁸ proposed a new analytical relation describing the rheological behavior of foam at a certain quality by introducing the “specific volume expansion ratio” (ratio of the liquid density to the foam density). Since most of the aqueous foams have been described as non-Newtonian fluids behaving as power-law fluid, with or without a yield stress, a power law seems therefore appropriate to describe foam behavior.³³

The description of both laminar and turbulent flow for both N₂ and CO₂ neat foams is separated in the work of Reindenbach *et al.*¹⁰ For evaluating laminar-flow pipe pressure losses, they assumed a yield pseudoplastic model dependent on foam quality, and defined an apparent viscosity:

$$\mu_a = \tau'_{yp} \left(\frac{8v}{D} \right)^{-1} + k' \left(\frac{8v}{D} \right)^{n-1}, \quad (2.2)$$

where the constants τ'_{yp} (approximate yield stress), k' (liquid consistency index), and n' (approximate flow behavior index) depend on geometry and are obtained from a plot of the wall-shear stress, τ_w , vs. shear strain, $8v/D$. To develop an explicit relationship to describe the rheology of foam, they suggested that these constants be replaced with the constants in Eq. 2.3 to 2.5, which don't depend on geometry but are constant for a particular fluid.

$$n' = n, \quad (2.3)$$

$$k' = k \left(\frac{4n}{3n+1} \right)^{-n}, \quad (2.4)$$

$$\tau'_{yp} = \tau_{yp} \left(\frac{3}{4} \right)^{-n}. \quad (2.5)$$

With these substitutions, they suggested that the resulting viscosity should be used as an apparent-Newtonian viscosity in standard pressure-drop calculations. Their turbulent flow model is based on the extension of the Melton and Malone³⁴ procedure but they incorporated an additional term to describe the varying foam density:

$$\frac{D\Delta p}{4L} = A' \rho_f^x d^e \left(\frac{8v}{D} \right)^{m'} , \quad (2.6)$$

where e , m' , and x are the diameter exponent, turbulent flow slope, and density exponent respectively.

For Newtonian fluids, values of the exponents e , m' , and x were found to be 1.6, 1.8, and 0.8 respectively. For hydroxypropyl guar (HPG) solutions and N₂ gas the relations between the exponents were found:

$$x = m' - 1, \quad (2.7a)$$

and

$$e = m'. \quad (2.7b)$$

2.4 Fluid Length Tracking

During matrix-acidizing treatments (where different stimulation fluids are injected along with foam down the wellbore), to accurately estimate the bottomhole pressure, each fluid *injected length* should be tracked as it flows down the wellbore. The compressible nature of foam would make the length of the fluid column decrease as it flows down the wellbore. This reduction in length, if not properly accounted for, can cause serious errors in estimating the bottomhole pressure. None of the previous analytical models^{1-5, 35} takes this into consideration. The method developed by Cullender and Smith³⁶ in estimating the wellbore pressure for gas was applied by Buslov and

Towler³⁵ in developing their iterative technique for the flow and flow-back of foam. Though they effectively tracked the foam column as it moved down the wellbore, they failed to account for the length reduction caused by pressure increase.

CHAPTER III

PRESSURE-DROP MODEL DEVELOPMENT

3.1 Overview

The development of the method to determine the bottomhole pressure for foams is presented in this chapter. General input to the program are surface and bottomhole treating temperatures, pipe diameter, pipe length, rheological parameters, surface treating pressure, injected flowrates, density of injected liquids, and gas/liquid ratio (GLR).

3.2 Analytical Model Development

Assuming an isothermal, one dimensional and steady-state flow, the mechanical energy balance for compressible foam flow in differential form is expressed as follow.¹⁶

$$\frac{v_f dv_f}{g_c} - \frac{g}{g_c} dZ + \frac{dp}{\rho_f} + 2 \frac{v_f^2 f_f}{Dg_c} dZ = 0 \quad (3.1)$$

An appropriate EOS and a rheological model that describes the viscosity and frictional factor of foam have to be developed before Eq. 3.1 can be solved.

3.2.1 Equation of State

The real or engineering gas law is used to describe the volumetric behavior of the gaseous phase. The gas density is expressed as

$$\rho_g = \frac{M_g p}{zRT}, \quad (3.2)$$

or

$$\hat{V}_g = \frac{zRT}{M_g p}, \quad (3.3)$$

where M_g and \hat{V}_g are the molecular weight and specific volume of gas respectively.

Assuming no-slip, the specific volume of foam can be written as

$$\hat{V}_f = \hat{V}_g (1 - \lambda_l) + \hat{V}_l \lambda_l, \quad (3.4)$$

where the no-slip holdup, λ_l , is expressed as

$$\lambda_l = \frac{q_l}{q_l + q_g}. \quad (3.5)$$

In Eq. 3.5 above, q_l and q_g are the in-situ liquid and gas flowrates. Substituting Eq. 3.3 into Eq. 3.4 results in

$$\hat{V}_f = (1 - \lambda_l) \frac{zRT}{M_g p} + \hat{V}_l \lambda_l. \quad (3.6)$$

By definition,

$$\hat{V}_f = \frac{1}{\rho_f}, \quad (3.7)$$

which can be written as

$$\hat{V}_f = \frac{a + bp}{p}, \quad (3.8)$$

where

$$a = (1 - \lambda_l) \frac{zRT}{M_g}, \quad (3.9)$$

and

$$b = \hat{V}_l \lambda_l. \quad (3.10)$$

3.2.2 Rheological Model

In their previous model, Reindenbach *et al.*¹⁰ assumed that the flow behavior index, n of the foam was equal to the base liquid value. Recognizing that the assumption was invalid at higher temperatures, they developed new empirical equations for both n and the foam consistency index, k_f to include temperature effects. They found out that the flow-behavior index of foam, n could be expressed as a function of temperature as³⁷

$$n_T = n \exp[(0.0028 - 0.0019\Gamma)(T - 75)], \quad (3.11)$$

where n_T and Γ are the temperature dependent flow-behavior index and foam quality respectively. The new temperature dependent liquid consistency index, k_T was modified and expressed as:

$$k_T = k_{75} \exp[(C_2\Gamma - 0.018)(T - 75)], \quad (3.12)$$

where k_{75} is the liquid consistency index at the reference temperature of 75°F given by Eq. 2.4, and C_2 is the foam-consistency-index exponent expressed as:

$$C_2 = \exp-(3.1 + 3n_T). \quad (3.13)$$

The consistency index of foam, k_f is then expressed as

$$k_f = k_T \exp[(C_1\Gamma - 0.75\Gamma^2)], \quad (3.14)$$

where C_1 , the foam-consistency-index exponent, is expressed as

$$C_1 = 4n_T^{1.8}. \quad (3.15)$$

Assuming a yield pseudoplastic model, the apparent viscosity of foam is expressed as

$$\mu_a = \tau'_{yp} \left(\frac{8v}{D} \right)^{-1} + k_f \left(\frac{8v}{D} \right)^{n_f-1}, \quad (3.16)$$

where τ'_{yp} , the yield point stress from approximate HB model, is a function of foam quality only. For $\Gamma \leq 0.6$

$$\tau'_{yp} = 0.07\Gamma \left(\frac{3}{4} \right)^{-n_T}, \quad (3.17)$$

and for $\Gamma > 0.6$,

$$\tau'_{yp} = 0.0002 \exp(9\Gamma) \left(\frac{3}{4} \right)^{-n_T}. \quad (3.18)$$

With proper representation of the viscosity, the next step is to determine the frictional factors for both laminar and turbulent flow regimes.

3.2.3 Pressure-Drop Model

Assume foam is injected down a pipe of cross-sectional area A_p and length L at depth $z = 0$, the mechanical energy balance equation is given by Eq. 3.1. The total mass flow rate, \dot{m}_t is

$$\dot{m}_t = \dot{m}_g + \dot{m}_l, \quad (3.25)$$

where \dot{m}_l and \dot{m}_g are the individual mass flowrates of liquid and gas respectively. From the definition of the continuity equation:

$$\dot{m}_t = \rho_f v_f A_p, \quad (3.26)$$

Expressing Eq. 3.26 in terms of the specific volume of foam, the average foam velocity is

$$v_f = \frac{\dot{m}_t \hat{V}_f}{A_p}. \quad (3.27)$$

Substituting Eq. 3.8 into Eq. 3.27 above

$$v_f = \frac{\dot{m}_t}{A_p} \left(\frac{a + bp}{P} \right) \quad (3.28)$$

and

$$dv_f = - \left(\frac{\dot{m}_t a}{A_p p^2} \right) dp \quad (3.29)$$

Substituting Eqs. 3.8, 3.28 and 3.29 into the mechanical energy equation, we obtain

$$\left[\frac{\dot{m}_t}{g_c A_p} \left(\frac{a + bp}{p} \right) \times \left(- \frac{\dot{m}_t a}{A_p p^2} dp \right) \right] - \frac{g}{g_c} \sin \theta dl + \left(\frac{a + bp}{p} \right) dp$$

$$+ \frac{2f_f}{Dg_c} \left[\frac{\dot{m}_t}{A_p} \left(\frac{a+bp}{p} \right) \right]^2 dl = 0, \quad (3.30)$$

where $dZ = \sin \theta dl$, and θ is the angle of deviation from the horizontal plane. To solve Eq. 3.30, an explicit expression for f_f as a function of L is required. But since no analytical expression exist for f_f as a function L , very small length increments will be taken to ensure a very small or constant friction factor. Therefore, f_f in Eq. 3.30 can be treated as a constant, Rearranging Eq. 3.30 gives:

$$\left[\frac{bg_c A_p^2 p^3 + ag_c A_p^2 p^2 - \dot{m}_t^2 abp - (\dot{m}_t a)^2}{(Dg_c A_p^2 \sin \theta - 2\dot{m}_t^2 f_f b^2) p^3 - 4ab\dot{m}_t^2 f_f p^2 - 2(\dot{m}_t)^2 f_f p} \right] dp = \frac{dl}{D}. \quad (3.31)$$

The integral of the above equation from inlet (surface) to outlet (bottomhole) yields,

$$(P_2 - P_1) + N_1 \ln \frac{P_2}{P_1} + N_2 \ln \left(\frac{P_2 - \alpha_1}{P_1 - \alpha_1} \right) + N_3 \ln \left(\frac{P_2 - \alpha_2}{P_1 - \alpha_2} \right) = K \frac{l}{D} \quad (3.32)$$

where,

$$\left. \begin{aligned} \alpha_1 &= \frac{w_1}{2} - \left[\left(\frac{w_1}{2} \right)^2 - w_2 \right]^{1/2} \\ \alpha_2 &= \frac{w_1}{2} + \left[\left(\frac{w_1}{2} \right)^2 - w_2 \right]^{1/2} \end{aligned} \right\}, \quad (3.33a)$$

$$\left. \begin{aligned}
 N_1 &= -\frac{w_3}{\alpha_1 \alpha_2}, \\
 N_2 &= \frac{\alpha_1^2 w_4 + w_5 \alpha_1 - w_3}{\alpha_1 (\alpha_1 - \alpha_2)}, \\
 N_3 &= \frac{\alpha_2^2 w_4 + w_5 \alpha_2 - w_3}{\alpha_2 (\alpha_2 - \alpha_1)},
 \end{aligned} \right\} \quad (3.33b)$$

$$K = \frac{(DgA_p^2 \sin \theta - 2\dot{M}_t^2 fb^2)}{A_p^2 bg_c}, \quad (3.33c)$$

and

$$\left. \begin{aligned}
 w_1 &= \frac{4a(b\dot{m}_t)^2 f_f + (aDgA_p^2 \sin \theta - 2a(b\dot{m}_t)^2 f_f)}{(DgA_p^2 b \sin \theta - 2bf_f (b\dot{m}_t)^2)}, \\
 w_2 &= \frac{2g_c (aA_p \dot{m}_t)^2 f_f + a\dot{m}_t (DgA_p^2 \sin \theta - 2f_f (b\dot{m}_t)^2)}{g_c A_p^2 (DgA_p^2 \sin \theta - 2f_f (b\dot{m}_t)^2)}, \\
 w_3 &= \frac{(a\dot{m}_t)^2}{g_c b A_p^2}, \\
 w_4 &= \frac{4ab\dot{m}_t^2 f_f}{(DgA_p^2 \sin \theta - 2f_f (b\dot{m}_t)^2)}, \\
 w_5 &= \frac{2f_f (a\dot{m}_t)^2}{(DgA_p^2 \sin \theta - 2f_f (\dot{m}_t b)^2)},
 \end{aligned} \right\} \quad (3.33d)$$

3.3 Friction Factor

For laminar flow, the frictional factor for foam is represented by the Fanning friction factor

$$f_F = \frac{16}{N_{RE}}, \quad (3.19)$$

where N_{RE} is the Reynolds number expressed in field units as

$$N_{RE} = \frac{1.48\rho_l q_t}{\mu_a D}. \quad (3.20)$$

where q_t is in *bbl/day*, ρ_l is in *lbm/ft³*, D in *in.*, and the apparent viscosity, μ_a obtained from Eq. 3.15 is in *cp*. For turbulent flow, the friction factor is obtained through the scale-up procedure provided by Reindenbach *et al.*¹⁰ By definition, the frictional factor is defined as

$$f = \frac{\tau_w}{\frac{1}{2}\rho_f v^2}, \quad (3.21)$$

where the wall shear stress, τ_w is equivalent to the expression in Eq. 2.6. Substituting Eq. 2.6 into Eq. 3.20 above, and rearranging gives

$$f' = 2^{3m'+1} \times A' \times \rho_f^{x-1} \times v^{m'-2} \times D^{e-m'}, \quad (3.22)$$

where A' is the modified turbulent scale-up parameter incorporating the liquid viscosity effect. The next problem is how to explicitly establish the transition from laminar to turbulent flow. This transition is normally obtained by the definition of a critical velocity, but this can't be developed explicitly for foams; therefore, Reindenbach *et al.*¹⁰

suggested that the frictional pressure drop, Δp_f for both flow regime be calculated.

Thus, for laminar flow, this is calculated from:

$$\Delta p_f = \frac{2f_f \rho_f v^2 l}{g_c D}, \quad (3.23)$$

and based on the modified scale-up relationship, the frictional pressure drop in turbulent flow is obtained from:

$$\Delta p_f = 4 \times A' \times \rho_f^x \times D^{e-1} \times \left(\frac{8v}{D} \right)^{m'} l. \quad (3.24)$$

The largest frictional pressure drop obtained would be the dominant flow regime. Then the corresponding friction factor can be obtained with either Eq. 3.19 or 3.22, depending on whether it is laminar or turbulent flow.

3.4 Fluid-Length Tracking

To accurately model the bottomhole pressure during a multi-stage acidizing treatment, two assumptions are made:

- Fluids are treated as either compressible or incompressible fluid columns
- No mixing occurs between different fluids during injection
- Linear temperature distribution along the wellbore length

The cross-sectional area of the tubing is

$$A_p = \frac{\pi D^2}{4}. \quad (3.34)$$

The total injection flowrate, q_t is

$$q_t = q_g + q_l, \quad (3.35)$$

where q_l and q_g are the in-situ liquid and gas flowrates respectively. For liquids, this is constant, but for gases, the in-situ flowrate is give by

$$q_g = 0.0283 \times q_l \times (GLR) \times \frac{T}{p}, \quad (3.36)$$

where q_g is in ft^3/min and GLR is the gas-liquid ratio. The fluid injected length after a certain time interval Δt is:

$$l_i = \frac{(q_t \times \Delta t)}{A_p}. \quad (3.37)$$

If the injected fluid i is incompressible, the Reynolds number in field unit is obtained from

$$N_{RE} = \frac{1.48 \rho_l q_t}{\mu_l D}, \quad (3.38)$$

where μ_l is the viscosity of the liquid. If $N_{RE} > 2100$, this implies turbulent flow and the friction factor is obtained from Chen's equation³⁸

$$f_f = \left\{ -4 \log \left[\frac{\varepsilon}{3.7065} - \frac{5.0452}{N_{RE}} \log \left(\frac{\varepsilon^{1.1098}}{2.8257} + \left(\frac{7.149}{N_{RE}} \right)^{0.8981} \right) \right] \right\}^{-2}, \quad (3.39)$$

else

$$f_f = \frac{16}{N_{RE}}. \quad (3.40)$$

For incompressible fluid, Eq. 3.32 reduces to the well known Fanning pressure drop equation:

$$(P_2 - P_1) - \frac{g}{g_c} \rho_l l_i \sin \theta + \frac{2f\rho_l v^2 l_i}{g_c D} = 0, \quad (3.41)$$

which is used to obtain the pressure at the bottom of fluid i . If the next injected fluid is compressible (foam), then from the assumption of linear temperature distribution, the temperature at any point down the fluid column length, l_{i+1} is given as

$$T = T_{surf} + \frac{(T_{bh} - T_{surf})}{L} l_{i+1} \sin \theta, \quad (3.42)$$

where l_{i+1} is the desired fluid column length or wellbore segment. The average temperature, T_{av} , over a fluid column or wellbore segment is given as:

$$T_{av} = T_{top} + \frac{(T_{bottom} + T_{top})}{2}, \quad (3.43)$$

where T_{top} and T_{bottom} are the top and bottom temperatures of the fluid column respectively obtained from Eq. 3.42. The in-situ quality of foam is given as

$$\Gamma = \frac{V_g}{V_g + V_l}, \quad (3.44)$$

where V_l and V_g are the corresponding volumes of liquid and gas injected give by

$$V_l = q_l \times \Delta t, \quad (3.45)$$

and

$$V_g = q_g \times \Delta t. \quad (3.46)$$

The viscosity of foam is estimated by the rheological equations presented earlier in section 3.2.2. With the viscosity of foam, the Reynolds number is obtained from Eq. 3.19. Assuming an appropriate length segment, Δl_{i+1} , a corresponding pressure drop across that foam segment is assumed:

$$(\Delta p)_{assumed} = 1\%(p_1), \quad (3.47)$$

and the corresponding average segment pressure

$$p_{av} = p_1 + \frac{(\Delta p)_{assumed}}{2}. \quad (3.48)$$

where p_1 is the pressure at the top of the fluid column. The gas compressibility factor used in calculating the gas density is obtained through the Beggs and Brill³⁹ (and later Standing⁴⁰) correlation. The pseudocritical pressure, p_{pc} and temperature, T_{pc} are first obtained from

$$p_{pc} = 709.6 - 58.7\gamma_g, \quad (3.49)$$

$$T_{pc} = 170.5 - 307.3\gamma_g, \quad (3.50)$$

where γ_g is the specific gas gravity. The corresponding pseudoreduced pressure and temperature are given as:

$$p_{pr} = \frac{p_{av}}{p_{pc}}, \quad (3.51)$$

$$T_{pr} = \frac{T_{av}}{T_{pc}}. \quad (3.52)$$

The gas compressibility factor, z is then obtained from

$$z = A^* + (1 - A^*)\exp(-B') + C'p_{pr}^{D'}, \quad (3.53)$$

where

$$\begin{aligned}
 A^* &= 1.39(T_{pr} - 0.92)^{0.5} - 0.36T_{pr} - 0.101, \\
 B' &= p_{pr} (0.62 - 0.23T_{pr}) + p_{pr}^2 \left[\frac{0.066}{(T_{pr} - 0.86)} - 0.037 \right] \\
 &\quad + \frac{0.32 p_{pr}^6}{\exp[20.723(T_{pr} - 1)]} \\
 C' &= 0.132 - 0.32 \log T_{pr}, \\
 D' &= \exp(0.715 - 1.128T_{pr} + 0.42T_{pr}^2).
 \end{aligned} \tag{3.54}$$

and

The gas Formation Volume Factor (FVF), B_g in scf/ft^3 is calculated from

$$B_g = 0.0283 \frac{zT_{av}}{P_{av}}. \tag{3.55}$$

The in-situ gas density is then calculated from Eq. 3.2, while the superficial liquid and gas velocities are obtained from their respective flowrates

$$v_{sl} = \frac{q_l}{A_p}, \tag{3.56}$$

and

$$v_{sg} = \frac{q_g}{A_p}. \tag{3.57}$$

The corresponding in-situ foam velocity is

$$v_f = v_{sl} + v_{sg}. \tag{3.58}$$

The mass flowrates are obtained from

$$\dot{m}_l = q_l \times \rho_l, \quad (3.59)$$

and

$$\dot{m}_g = q_g \times \rho_g. \quad (3.60)$$

The corresponding foam density is calculated from

$$\rho_f = \rho_l \lambda_l + \rho_g (1 - \lambda_l). \quad (3.61)$$

Now the flow regime (laminar or turbulent) has to be established. This is carried out according to the procedure outlined in section 3.2.2. If the flow is laminar, then the friction factor used for the bottomhole pressure calculation is given by Eq. 3.19 as

$$f_f = \frac{16}{N_{RE}},$$

else Eq. 3.22 is used

$$f_f = 2^{3m'+1} \times A' \times \rho_f^{x-1} \times v^{m'-2} \times D^{e-m'}.$$

Once the flow regime has been established and the corresponding friction factor has been calculated, the constants from Eq. 3.33 are calculated and Eq. 3.32 is solved iteratively to obtain the pressure at the bottom of the fluid length segment. If this pressure is at least 10% greater than the pressure assumed, the whole process is repeated until the difference between the calculated and assumed pressure is negligible.

This final pressure then becomes the pressure at the top of the next fluid length segment, and the calculations are repeated until the sum of all the fluid length segments equals the length of the injected fluid. The pressure at the bottom of the last segment

then becomes the pressure at the top of the previous injected fluid. Then the whole pressure drop calculation is repeated for the previous fluid.

This process is repeated for any number of fluids and the corresponding bottomhole pressure value is obtained. An arbitrary example illustrating the tracking of the fluids injected length (including foam) during an acidizing treatment is given in Appendix A.

CHAPTER IV

SKIN FACTOR EVOLUTION IN MATRIX ACIDIZING

4.1 Overview

Generally, skin effect is an additional pressure drop that occurs in the near-wellbore region. This effect could either be positive or negative, depending on the mechanism involved. Additionally, the skin effect characterizes the damage around a well. During a stimulation treatment, skin evolution can be used to evaluate the effectiveness of the treatment. It directly indicates if the injection is removing the damage or not. This chapter illustrates how to calculate the skin factor during a stimulation treatment from the bottomhole pressure and flowrate.

4.2 Matrix-acidizing Evaluation

Real-time monitoring is an effective way of optimizing matrix-acidizing treatments¹⁻⁵ particularly in assisting operators to determine when the optimum volume of acid has been injected. It is based on the evaluation of the bottomhole pressure and flowrate, from which the evolving skin factor is determined. This computed skin factor provides several benefits:

- It provides a quantitative measure of the effectiveness of the overall stimulation treatment.
- The observed skin-factor trend can be used to alter the treatment design based on actual response to eliminate damages caused by any fluid injection.

- It enables the effectiveness of individual fluid stages pumped during the treatment to be evaluated.

The different techniques for evaluating matrix-acidizing treatment presented in literature can be grouped into two groups; steady-state and transient models. Paccoloni and Tambini⁴¹ applied the steady-state, radial-flow form of Darcy's law to monitor the progress of a stimulation treatment, by evaluating the skin factor, s given by:

$$s = \frac{0.00708kh(p_{wf} - p_e)}{\mu q_i} - \ln \frac{r_b}{r_w}, \quad (4.1)$$

where r_w is the wellbore radius and r_b is the radius affected by the injection of acid and they suggested a value of 4 ft to be used. Prouvost and Economides^{42, 43} pointed out that the above technique overestimates the skin factor and does not account for the pressure response as a result of rate changes. They then presented an alternative technique to predict the skin factor with higher accuracy, by simulating the transient pressure response that would occur for the particular injection rate schedule. The major drawback to this method is the need for a fast simulator, and the prior knowledge of the injection schedule, which limits its real-time evaluation application.

Hill and Zhu^{44, 45} developed an alternative skin factor technique that draws on both Paccoloni⁴¹ and Prouvost and Economides^{42, 43} methods. The line source solution for transient flow during injection is approximated as⁴⁶:

$$\frac{p_{wf} - p_i}{q_i} = \frac{162.6B\mu}{kh} \left[\log t + \log \left(\frac{k}{\phi \mu c_t r_w^2} \right) - 3.23 + 0.86859s \right], \quad (4.2)$$

Where B, c_i, h, k, p_i and ϕ are defined as the Formation Volume Factor (FVF), reservoir compressibility, thickness, permeability, initial pressure, and porosity respectively. To accommodate for varying flowrates, Eq. 4.2 can be re-arranged by applying the principle of superposition to give^{44, 45}

$$\frac{p_i - p_{wf}}{q_N} = m_c \sum_{j=1}^N \left[\frac{(q_j - q_{j-1})}{q_N} \log(t - t_{j-1}) \right] + b', \quad (4.3)$$

where the slope, m_c is constant during an acid treatment, and is given as

$$m_c = \frac{162.6B\mu}{kh} \quad (4.4)$$

and the intercept, b' is

$$b' = m_c \left[\log \left(\frac{k}{\phi \mu c_t r_w^2} \right) - 3.2275 + 0.86859s \right]. \quad (4.5)$$

They then introduced the *superposition time*, Δt_{sup} function, and expressed Eq. 4.3 as

$$\frac{p_i - p_{wf}}{q_N} = m_c \Delta t_{\text{sup}} + b', \quad (4.6)$$

where

$$\Delta t_{\text{sup}} = \sum_{j=1}^N \frac{(q_j - q_{j-1})}{q_N} \log(t_N - t_{j-1}). \quad (4.7)$$

The superposition time defined above, handles multiple flowrate injection and removes the effect of flowrate change on the pressure response; thus the resulting pressure curve represent only effects from skin factor changes.

From Eq. 4.6, a plot of inverse injectivity vs. the superposition time function, Δt_{sup} would give a straight line with a constant slope, m_c and intercept, b' that depends on the skin factor at that point. The intercept, b' , can be calculated from the measured bottomhole pressure and injection rate, then the skin factor can easily be determined from the intercept. When the surface pressure is measured, rather than the bottomhole pressure, the bottomhole pressure in Eq. 4.6 is calculated by the method presented in chapter III. Solving for the skin factor from Eq. 4.5 gives

$$s = 1.152 \left[\frac{b'}{m_c} - \log \left(\frac{k}{\phi \mu c_t r_w^2} \right) + 3.23 \right]. \quad (4.8)$$

CHAPTER V

DEVELOPMENT OF PROGRAM FOR BOTTOMHOLE

PRESSURE CALCULATION

5.1 Program Outline

Based on the methodology described in Chapter III, a program was developed using Visual Basic (VB) for calculating the bottomhole pressures for stimulating fluids including foams. A simplified flow chart describing the operational sequence of the program is shown in **Fig. 5.1**.

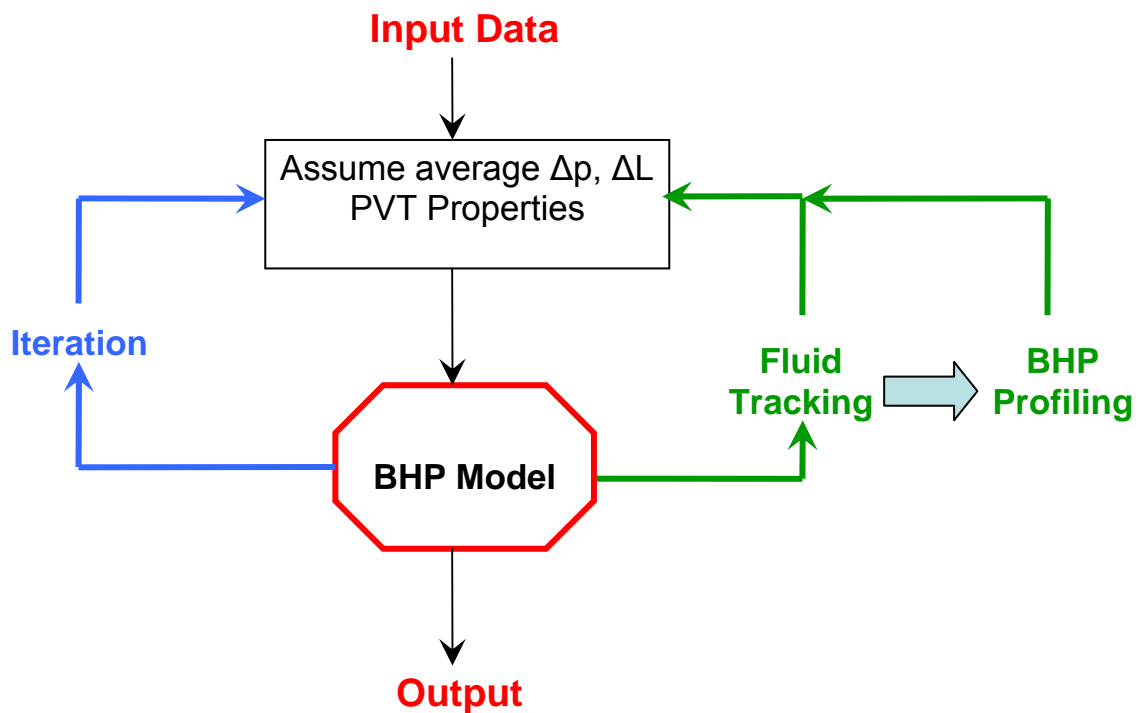


Fig. 5.1—Flow chart for estimating the bottomhole pressure (BHP) for stimulating fluids including foam.

The program treats all fluids as either incompressible or compressible. For foams, it takes the inputted rheological parameters (for both its gaseous and liquid phases) and uses its own subroutine to calculate the viscosity and the corresponding frictional factor as described in section 3.2.2.

The program calculates the bottomhole pressure for any pipe deviation. It uses surface and bottomhole treating temperatures, pipe diameter, total pipe length, surface treating pressure and injected flowrates, density of injected liquids, and gas/liquid ratio (GLR) to output the bottomhole pressure, flowrate, and corresponding fluid at the perforation.

5.2 Model Validation

Before the program can be applied to matrix acidizing, it needs to be verified for the flow of foam only. There is a dearth of “clean” data for neat-foam flow, nevertheless, two cases were found and are present here.

For the first case, the input data (inlet flowrate and pressure, pipe length and diameter) were taken from a single test run from Schramm⁴⁷. Rheological parameters were from Reindenbach *et al.*¹⁰ N₂ foam was injected down a 5.5” pipe to a depth of 4602 ft. The bottomhole pressure measured at that depth was reported as 4,492 psi. Using Eq. 3.32, a bottomhole pressure of 4,592 psi was obtained for this condition; which is a difference of 2%.

The second case represents a field treatment performed and reported by Lord¹⁴. It involved the injection of N₂ foam down the tubing/casing annulus. Treatment details are

shown in **Table 5.1**, while **Table 5.2** compares the predicted BHP with the actual field BHP below.

Parameter	Value
Casing diameter, <i>in</i>	5.512
Casing length, ft	9403
Design foam quality	0.65
Liquid density, lbm/ft ³	63.58
Liquid flowrate, bpm	4.00
Surface temperature, F	82.4
Tubing diameter, <i>in</i>	2.362
Tubing length, ft	9620

Job Time	Surface pressure	Actual BHP	Predicted BHP	Deviation from
min	psi	psi	psi	actual, %
18	3775	4843	4422	8
28	3755	4791	4353	9
44	3755	4860	4319	11
86	4276	5630	4880	13
96	4664	6182	5300	14
104	4815	6572	5425	17

From **Fig. 5.2**, it is observed that the presence of solids (proppants) somewhat affects the accuracy of the predicted BHP value. For low proppant concentration, the predicted BHP gives a good match with the measured BHP, but as the proppant concentration increases, the accuracy of the predicted result decreases. This is due to two factors; first, the presence of proppants was neglected in the formulated EOS, and second the rheological model applied was developed for the flow of neat foams without any consideration to the presence of solids or proppants. To properly account for the

presence of proppant, an additional proppant term would have to be incorporated into the EOS, which will result in an increase in the overall density of foam. This would produce higher pressure drop or bottomhole pressure values.

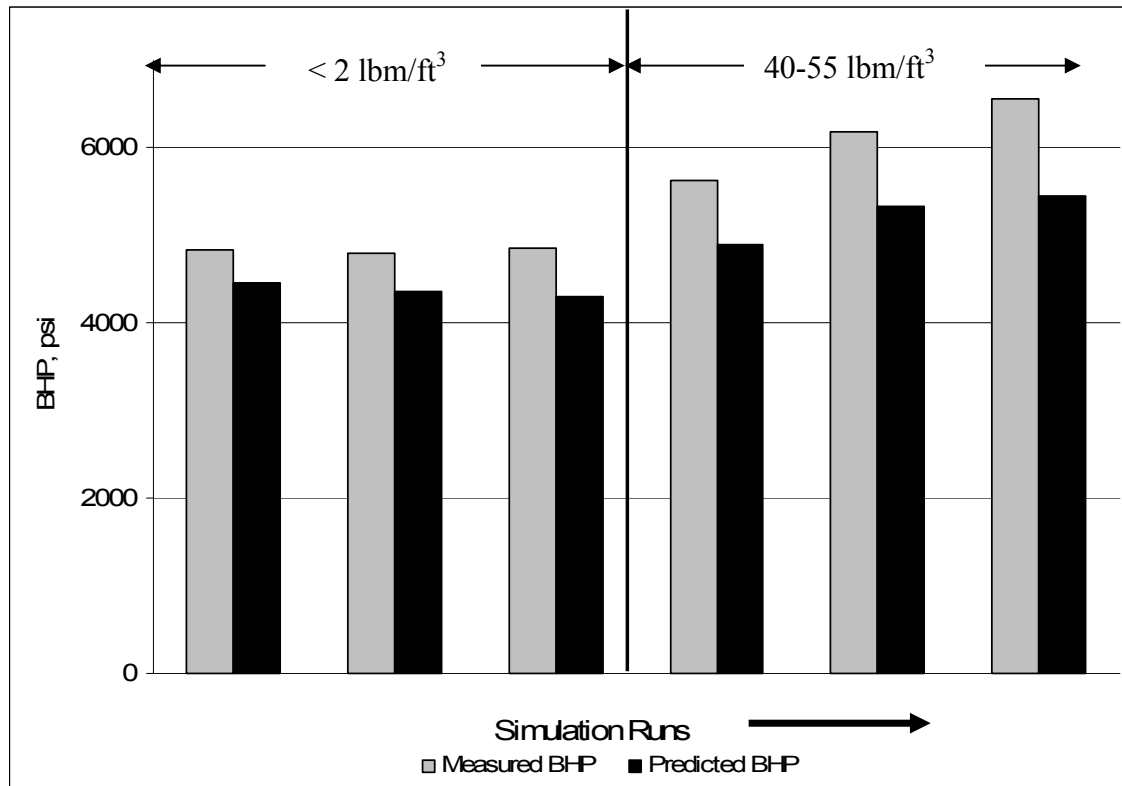


Fig. 5.2—Effect of proppant on predicted BHP.

Furthermore, in this case, foam was injected down the tubing/casing annulus, but the rheological model used was not formulated for annular flow. To overcome this, a *hydraulic diameter* (difference between casing and tubing diameter) was used.

Based on the foregoing comparisons, it states that the new model is valid for neat foam hydraulics calculations. Further validation is certainly desirable if more accurate field data are available in the future.

CHAPTER VI

FIELD APPLICATION EXAMPLES

6.1 Matrix-acidizing Stimulation Examples

One matrix-acidizing treatment is presented here to show how to use measured surface pressure and flowrate to evaluate acid stimulation on-site. The field example involved the eight repetitive injection sequence of different fluids separated by a nitrogen diversion stage as shown in **Table 6.1**.

TABLE 6.1— FLUID TREATMENT SCHEDULE FOR FIELD EXAMPLE.		
Stage No.	Fluid	Stage Volume, bbl
1	Xylene	8.2
2	5% NH ₄ CL	12.4
3	10% HCL	12.4
4	Mud acid	31.0
5	5% HCL	12.4
6	Diverter (N ₂ Foam)	30.0

The initial skin factor of this well was 19.7 and since both viscosity, μ and Formation Volume factor (FVF), B , were not given, their product, μB , was selected to match the initial skin factor during the early injection stages. **Fig. 6.1** shows the field surface pressure and injection rate history.

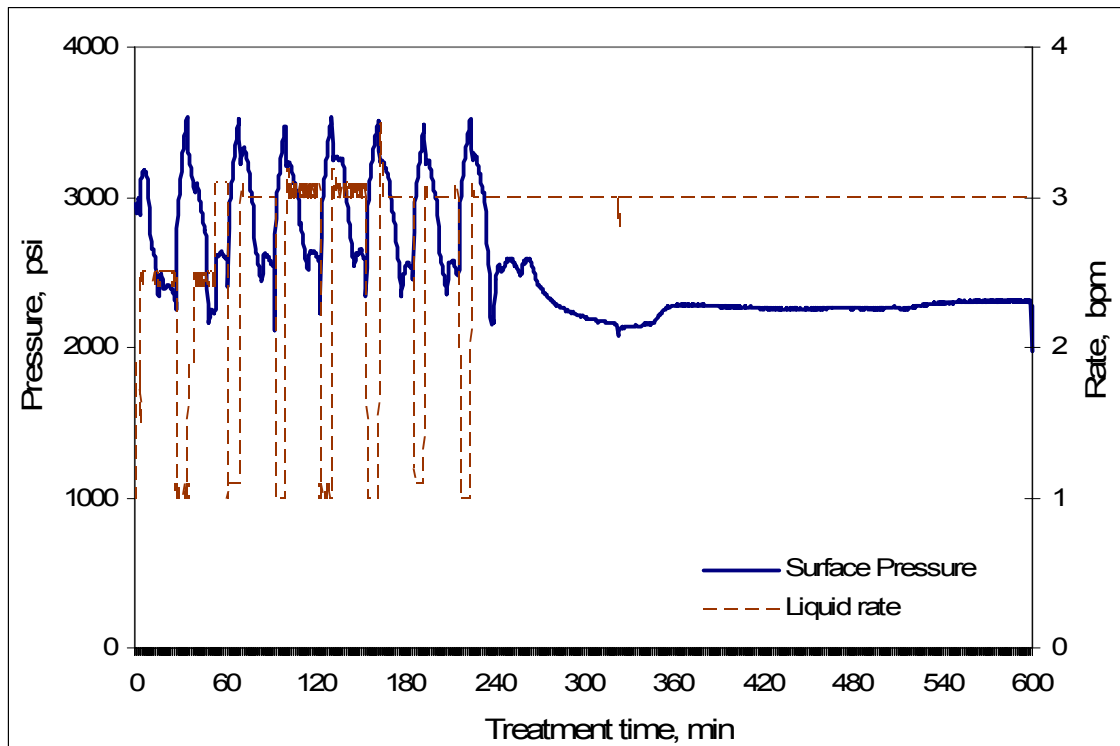


Fig. 6.1—Field treatment history.

A unique thing about this particular treatment is that analysis of the surface treating pressure can be carried out because the wellbore contained the same fluid volumes which were pumped at the same rate. A couple of good places to carry out this analysis are just before and after the nitrified diverter stages as shown in **Fig 6.2**.

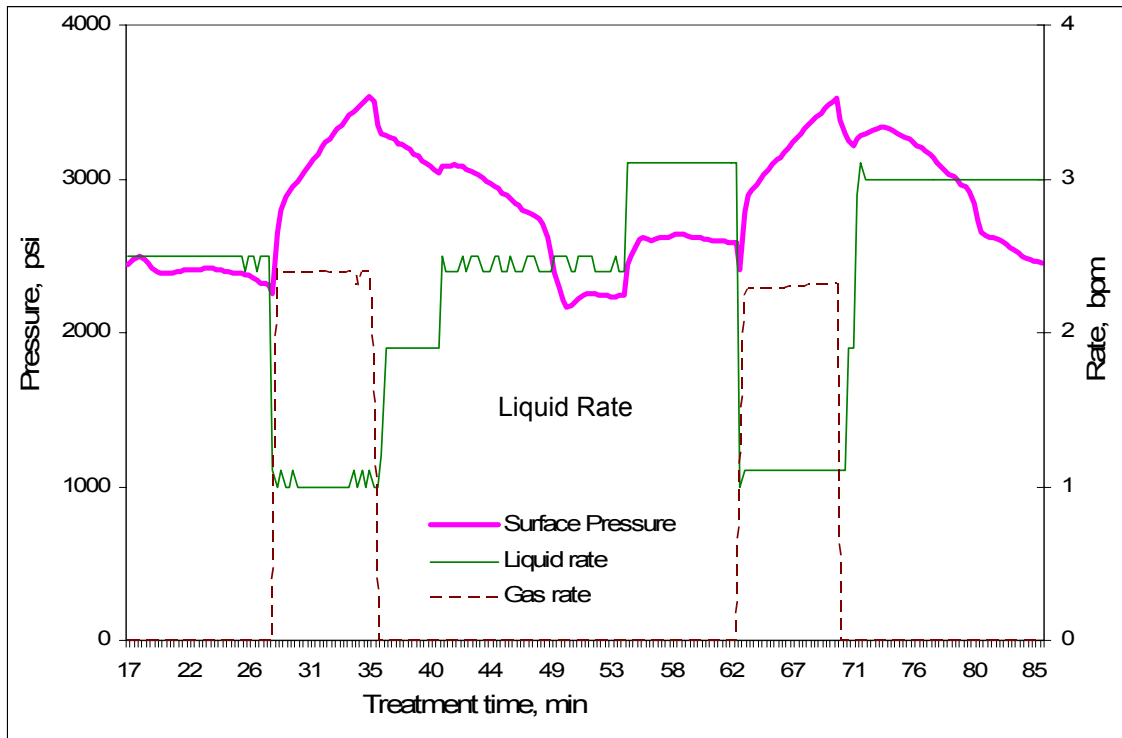


Fig. 6.2—Cut-out section of the field treatment history used for analysis.

The calculated BHP profile from the measured surface pressure by the method presented before is shown in **Fig 6.3**. There is relatively no increase in the BHP when the diverter (foam) gets to the perforation as observed from Fig 6.3; which implies that the nitrified diverter stage was ineffective. The BHP before and after the treatment is almost the same implying that little or no stimulation was achieved after the treatment.

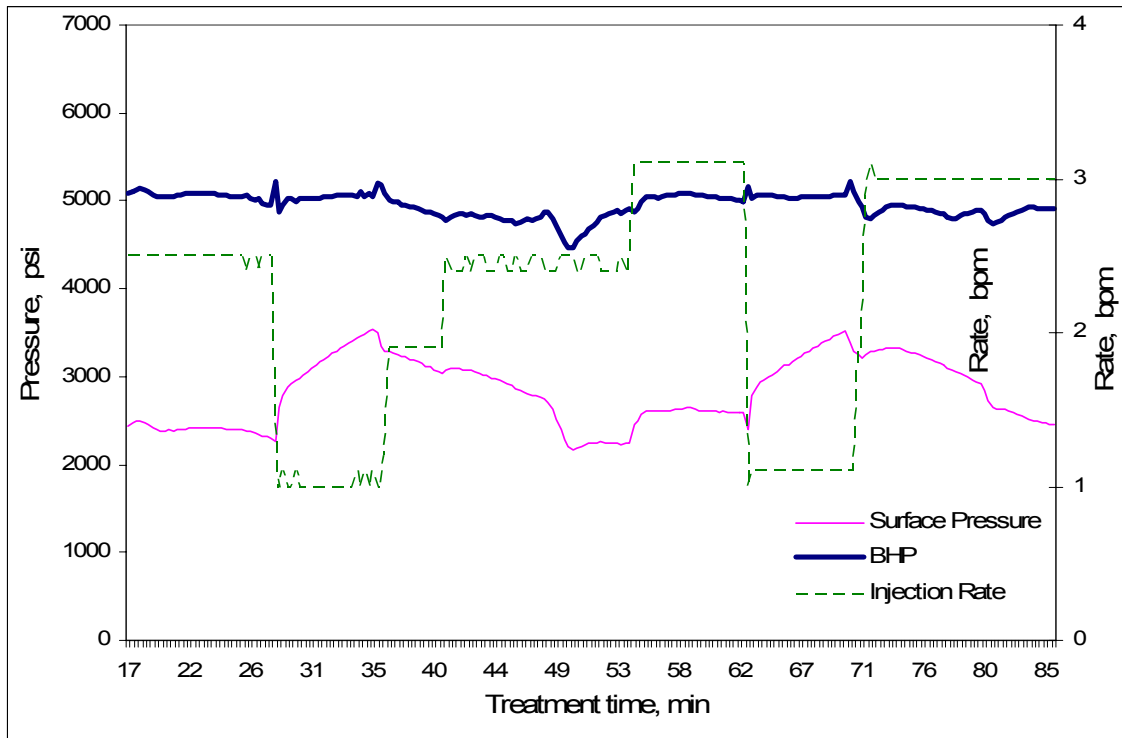


Fig. 6.3—Bottomhole pressure and injection rate history for field example.

The corresponding skin factor evolution is shown in **Fig. 6.4**. From it, we can see It has a slight decreasing trend with the skin factor before and after the treatment almost the same. This implies that little stimulation was achieved; which corresponds to the almost constant BHP shown previously in Fig 6.3.

There is also little increase in the apparent skin factor when the diverter (foam) is at the perforation, seen on Fig 6.4, and it indicates ineffective or no diversion by the foam during the injection.

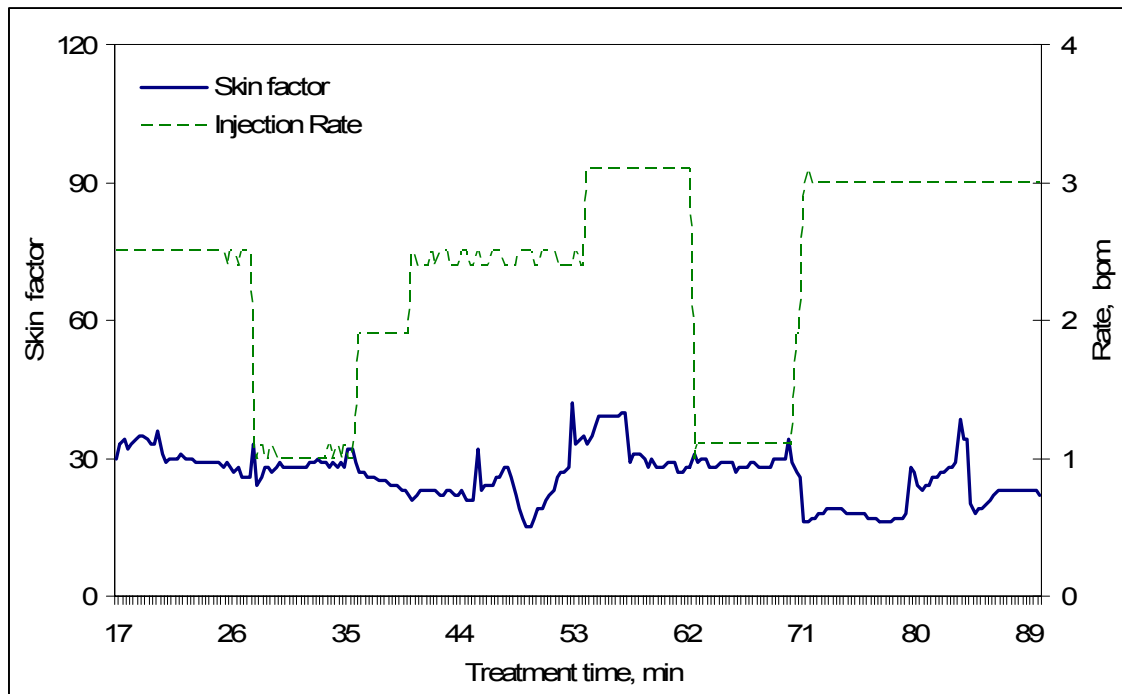


Fig. 6.4—Calculated skin factor history.

6.2 Tracking Injected-Fluid Length

An arbitrarily example is presented below to show the effect of fluid-volume reduction, because of the compressibility of gas, on the calculated BHP. The treating schedule is shown in **Table 6.2** below. It involves the injection of foam into the wellbore initially filled with brine, and then the total displacement of foam by brine to fill-up the wellbore. The entire treatment was performed at constant surface pressure to facilitate better BHP analysis.

TABLE 6.2—FLUID TREATMENT SCHEDULE FOR ARBITRARY EXAMPLE.	
Stage No.	Fluid
1	Brine
2	Foam Diverter
3	Brine

Fig. 6.5 compares the BHP profile when the volume reduction and fluid tracking of the diverter stage are accounted for and neglected. It can be seen from Fig. 6.5 that neglecting the volume reduction of the foam diverter produces a lower estimated BHP. During the injection of the foam at the surface, little or no difference is seen in the calculated BHP. But as the displacement of foam down the wellbore begins, a difference in the calculated BHP can be observed. This difference increases and reaches its maximum when the foam gets to the perforation. During the displacement of foam into the formation, there is relatively no difference in the calculated BHP. This difference in the calculated BHP could increase depending on the wellbore and actual treatment conditions.

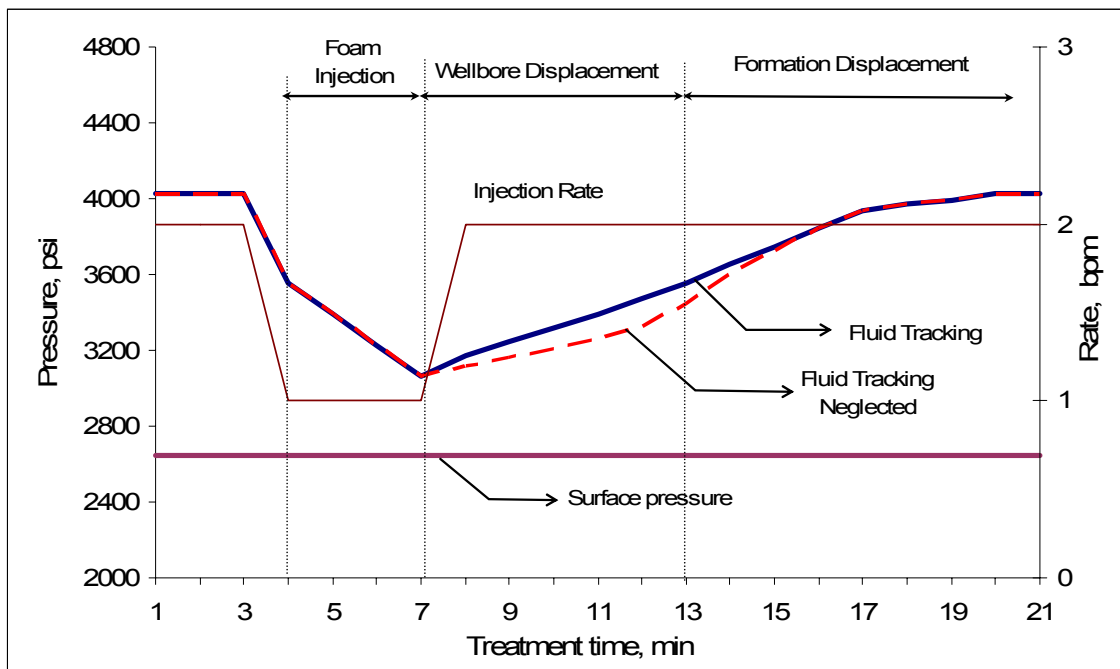


Fig 6.5—Effect of foam volume reduction on the estimated BHP.

The fluid tracking process results in a decrease in the volume of foam in the wellbore due to increase in pressure. Additionally, since neat foam has a significant lower density compared to brine, a higher BHP would be obtained; compared to when the wellbore is filled with a large volume of foam resulting in a lower BHP value.

CHAPTER VII

CONCLUSIONS AND RECOMMENDATIONS

7.1 Conclusions

Based on the results of the preliminary tests, the developed program accurately describes the pressure behavior for the flow of neat foams only.

The program is flexible and can readily be incorporated into an appropriate skin factor model to perform either real-time or posttreatment skin factor analysis.

Neglecting the reduction of column length could cause significant differences in the predicted BHP values depending on the quality of foam; and this can result in errors in the skin factor evaluation.

7.2 Recommendations

Further testing of this program using accurate field data is highly recommended. Then, it can confidently be incorporated for real-time skin factor monitoring purposes.

The reduction of column length should be thoroughly investigated, with a wide range of foam qualities.

Though the rheological model incorporated in the program handles both N_2 and CO_2 foams, field data containing CO_2 foams should be tested with the program to ensure similar accuracy.

NOMENCLATURE

A = pipe area, in²

A' = modified turbulent flow scale-up parameter, lbf-sec^m/lbm^xft^{e+2-3x}

b' = intercept of inverse injectivity versus Δt_{sup} plot for a vertical well, dimensionless

B = formation volume factor, dimensionless

$C_{1,2}$ = foam-consistency-index exponent, dimensionless

c_i = reservoir compressibility, psi⁻¹

D = pipe ID, in

e = diameter exponent, turbulent flow scale-up, dimensionless

f = friction factor, dimensionless

g = gravitational acceleration, ft/s²

h = reservoir thickness, ft

K = consistency index, lbf/ft²

K' = liquid consistency index, lbf-secⁿ/ft²

K_f = foam consistency index (HB model), lbf-secⁿ/ft²

K_{75} = consistency index of liquid phase at 75°F, lbf-secⁿ/ft²

l = segment length, ft

L = wellbore length, ft

m = mass, lbm

\dot{m} = mass flowrate, lbm/s

m_c = slope of inverse injectivity versus Δt_{sup} plot for a vertical well, dimensionless

M_g = molecular weight of gas, lb/lb-mole

\dot{M}_t = total mass flowrate, lbm.s

n = flow behavior index (pseudoplastic and HB models), dimensionless

n' = flow behavior index (approximate HB model), dimensionless

n_T = flow behavior index of liquid phase as a function of temperature, dimensionless

N_{RE} = Reynolds number, dimensionless

p = pressure, psi

p_e = pressure at drainage radius, psi

p_i = initial reservoir pressure, psi

p_{wf} = bottomhole pressure, psi

q_i = injection rate, bpm

r_b = radius affected by acid injection, ft

r_w = wellbore radius, ft

R = gas constant, psia.ft³/lbmR

s = skin factor, dimensionless

T = temperature, °F

v = velocity, ft/s

\widehat{V} = specific volume, ft³/lbm

W = mass fraction, dimensionless

x = turbulent flow correlation exponent, dimensionless

z = gas compressibility factor, dimensionless

Z = vertical elevation, ft

Δ = difference, dimensionless

Δp = pressure difference, psi

Δt_{sup} = superposition-time function, min

$\dot{\gamma}$ = shear rate, sec^{-1}

γ_g = specific gas gravity, dimensionless

Γ = foam quality, %

λ = no-slip holdup, dimensionless

ϕ = porosity, %

μ = viscosity, cp

μ_a = apparent viscosity, cp

ρ = density, lbm/ft^3

τ = shear stress, lbf/ft^2

τ_{yp} = true yield point stress, lbf/ft^2

τ'_{yp} = yield point stress from approximate HB model, lbf/ft^2

θ = pipe inclination from horizontal, $^\circ$

Subscripts

1 = Position 1, surface

2 = Position 2, bottomhole

bh = bottomhole

c = constant

f = foam

g = gas

j = counter

l = liquid

N = total number of injection rates, dimensionless

p = pipe

sg = superficial gas

sl = superficial liquid

t = total

T = temperature

w = wall

REFERENCES

1. Hill, A.D and Zhu, D.: "Real-Time Monitoring of Matrix Acidizing Including the Effects of Diverting Agents," paper SPE 28548 presented at the 1994 SPE Annual Technical Conference and Exhibition, New Orleans, 25-29 September.
2. Paccaloni, G. and Tambini, M.: "Advances in Matrix Stimulation Technology," *JPT* (March 1993) 256.
3. Prouvost, L.P. and Economides, M.J.: "Application of Real-Time Matrix Acidizing Evaluation Method," *SPEPE* (November 1989) 401.
4. Prouvost, L.P. and Economides, M.J.: "Real-Time Evaluation of Matrix Acidizing Treatments," *J. Pet. Sci. and Eng.* (1987) **1**, 145.
5. Behenna, F.R.: "Interpretation of Matrix Acidizing Treatments Using a Continuously Monitored Skin Factor," paper SPE 27401 presented at the 1994 SPE Formation Damage Control Symposium, Lafayette, Louisiana, 7-10 February.
6. Hill, A.D. and Rossen, W.R.: "Fluid Placement and Diversion in Matrix Acidizing," paper SPE 27982 presented at the 1994 Tulsa/SPE Centennial Petroleum Engineering Symposium, Tulsa, Oklahoma, 29-31. August.
7. Khatib, Z.I., Hirasaki, G.J., and Falls, A.H.: "Effects of Capillary Pressure on Coalescence and Phase Motilities in Foams Flowing Through Porous Media," *SPEPE* (August 1988) 919-926.
8. Heller, J.P. and Kuntamukka, S.: "Critical Review of the Foam Rheology Literature," *Ind. Eng. Chem. Res.*, (1987) **26**, 318.

9. Prud'homme, R.K. and Khan, S.A.: "Experimental Results on Foam Rheology, in Foams, Theory, Measurements and Applications," *Surfactant Science Series* (1996) **57**, 217.
10. Reindenbach, V.G., Harris, P.C., Lee, Y.N., and Lord, D.L.: "Rheological Study of Foam Fracturing Fluids Using Nitrogen and Carbon Dioxide," paper SPE 12026 presented at the 1983 SPE Annual Technical Conference and Exhibition, San Antonio, Texas, 5-8 October.
11. Krug, J.A. and Mitchell, B.J.: "Charts Help Find Volume, Pressure Needed for Foam Drilling," *Oil and Gas J.* (7 February 1972) 61.
12. Beyer, A.H., Millhone, R.S., and Foote, R.W.: "Flow Behavior of Foam as a Well Circulating Fluid," paper SPE 3986 presented at the 1972 SPE Annual Fall Meeting, San Antonio, Texas, 2-5 October.
13. Blauer, R.E., Mitchell, B.J., and Kohlhaas, C.A.: "Determination of Laminar, Turbulent and Transitional Foam-Flow Friction Losses in Pipes," paper SPE 4885 presented at the 1974 Annual California Regional Meeting, San Francisco, 4-5 April.
14. Lord, D.L.: "Analysis of Dynamics and Static Foam Behavior," *JPT* (January 1981) 39.
15. Blauer, R.E. and Kohlhaas, C.A.: "Formation Fracturing with Foam," paper SPE 5003 presented at the 1974 SPE Annual Fall Meeting, Houston, 6-9 October.
16. Bird, R.B., Stewart, W.E., and Lightfoot, E.N.: *Transport Phenomena*, John Wiley and Sons Inc., New York (1960).

17. Sporker, H.F., Trepess, P., Valko, P., and Economides, M.J.: "System Design for the Measurement of Down Hole Dynamic Rheology for Foam Fracturing Fluids," paper SPE 22840 presented at the 1991 Annual Technical Conference and Exhibition, Dallas, 6-9 October.
18. Valko, P. and Economides, M.J.: "Volume Equalized Constitutive Equations for Foamed Polymer Solutions," *J. of Rheology* (1992) **36**, 1033.
19. Okpobiri, G.A. and Ikoku, C.U.: "Experimental Determination of Friction Factors for Mist and Foam Drilling and Well Cleanout Operations," *J. of Energy Resources Technology* (1983) **105**, 542-553.
20. Nakagawa, E.Y. *et al.*: "Comparison of Aerated Fluids/Foam Drilling Hydraulics Simulators Against Field Data," paper SPE 54319 presented at the 1999 DPE Asia Pacific Oil and Gas Conference and Exhibition, Jakarta, Indonesia, 20-22 April.
21. Ozbayoglu, M.E., Kuru, E., Miska, S., and Takach, N.: "A Comparative Study of Hydraulic Models for Foam Drilling," paper SPE/Petroleum Society of CIM 65489 presented at the 2000 SPE/Petroleum Society of CIM international Conference on Horizontal Well Technology, Calgary, 6-8 November.
22. Ross, S.: "Bubbles and Foams," *Ind. Eng. Chem.* (1969) **61**, 48-55.
23. David, A. and Marsden, S.S. Jr.: "The Rheology of Foam," paper SPE 2544 presented at the 1969 SPE Annual Fall Meeting, Denver, 28 September-1 October.
24. Huey, C.T. and Bryant, R.A.A.: "Isothermal Homogeneous Two-phase Flow in Pipes," *AIChE J.* (1967) **13**, 70-81.

25. Raza, S.H. and Marsden, S. S.: "The Streaming Potential and the Rheology of Foam," *SPEJ* (March 1967) 359.
26. Patton, J.T., Holbrook, S.T., and Hsu, W.: "Rheology of Mobility-Control Foams," *SPEJ* (1983) 456.
27. Sanghai, V. and Ikoku, C.U.: "Rheology of Foam and its Implications in Drilling and Cleanout Operations," *J. of Energy Resources Technology* (1983) **105**, 362.
28. Thondavadi, N.N. and Lemlich, R.: "Flow Properties of Foam With and Without Solid Particles," *Ind. Eng. Chem. Process Des. Dev.* (1985) **24**, 748.
29. Enzendorfer, C., Harris, R.A., Valko P., Economides, M.J., and Fokker, P.A. *et al.*: "Pipe Viscometry of Foams," *J. of Rheology* (1995) **39**, No. 2, 345.
30. Khan, S.A., Schnepfer, C.A., and Armstrong, R.C.: "Foam Rheology: III. Measurement of Shear Flow Properties," *J. of Rheology* (1988) **32**, No. 1, 69.
31. Calvert, J.R. and Nezhati, K.: "Bubble Size Effects in Foams," *Int. J. Heat and Fluid Flow* (1992) **8**, No. 2, 102.
32. Burley, R. and Shakarin, M.: "An Experimental Study of Foam Rheology in Straight Capillary Tubes," *Eng. Fluid Mech.* (1992) **5**, No. 2, 115.
33. Herzhaft, B.: "Rheology of Foams: A Literature Review of Some Experimental Works," *Oil and Gas Science and Technology* (1999) **54**, No. 5, 587.
34. Melton, L.L. and Malone, W.T.: "Fluid Mechanics Research and Engineering Application in Non-Newtonian Fluid Systems," *SPEJ* (March 1964) **4**, 56.

35. Buslov, R. and Towler, B.F.: "Calculation of Pressure of Foams in Well Completion Processes," paper SPE 36490 presented at the 1996 Annual Technical Conference and Exhibition, Denver, Colorado, 6-9 October.
36. Cullender, M. H. and Smith, R.V.: "Practical Solution of Gas Flow Equations for Wells and Pipelines with Large Temperature Gradients," *Trans. AIME* (1956) **207**, 287.
37. Reindenbach, V.G. and Harris, P.C.: "High-Temperature Rheological Study of Foam Fracturing Fluids," paper SPE 13177 presented at the 1984 SPE Annual Technical Conference and Exhibition, Houston, 16-19 September.
38. Chen, N.H.: "An Explicit Equation for Friction Factor in Pipe," *Ind. Eng. Chem. Fund.*, (1979) **18**, 296.
39. Brill, J. P and Beggs, H. D.: *Two-Phase Flow in Pipes*. The Univ. of Tulsa, Tulsa, Oklahoma (1978).
40. Standing, M. B.: *Volumetric and Phase Behavior of Oil Filled Hydrocarbon Systems*, SPE of AIME, 8th Printing, New York (1977).
41. Paccaloni, G. and Tambini, M.: "Advances in Matrix Stimulation Technology," *JPT* (March 1993) 256-263.
42. Prouvost, L.P. and Economides, M.J.: "Applications of Real-Time Matrix Acidizing Evaluation Method," *SPEPE* (November 1989) 401-406.
43. Prouvost, L.P. and Economides, M.J.: "Real-Time Evaluation of Matrix Acidizing Treatments," *J. Pet. Sci. and Eng.*(1987) **1**, 145-154.

44. Hill, A.D. and Zhu, D.: "Real-Time Monitoring of Matrix Acidizing Including The Effects of Diverting Agents," paper SPE 28548 presented at the 1994 SPE Annual Technical Conference and Exhibition, New Orleans, 25-28 September.
45. Hill, A.D. and Zhu, D.: "Field Demonstrate Enhanced Matrix Acidizing Through Real-Time Monitoring," paper SPE 35197 presented at the 1996 Permian Oil and Gas Recovery Conference, Midland, Texas, 27-29 March.
46. Earlougher Jr., R.C.: *Advances in Well Test Analysis*, Monograph Series, SPE, Richardson, Texas (1977) **5**, 5.
47. Schramm, L.L.: *Foams: Fundamentals and Applications in the Petroleum Industry*, Advances in Chemistry Series (1994) **242**, 365.

APPENDIX A

FLUID TRACKING CALCULATIONS

An arbitrary example is used to illustrate the process of tracking injected length of fluids. For this example, three fluids (including foam) are used as shown in **Table A-1**. The corresponding well data are shown in **Table A-2**.

Fluid	Injected time min	P₁ psi	q_i bpm	GLR scf/bbl	liquid density lbm/ft³
Mud acid	3	2400	2	0	67
Foam	4	2400	1	1800	60
Brine	Fill up	2400	2	0	62.4

Parameter	Value
Bottomhole temperature, °F	172
Pipe inclination, °	56
Surface temperature, °F	82.4
Tubing diameter, <i>in</i>	2.259
Tubing length, ft	5000

Normally, before injection commences, the wellbore is filled with an inert fluid. Here it is assumed that the wellbore is filled with Brine (density= 62.4 lbm/ft³). Thus, for the first injection stage (Mud acid):

Pipe area is

$$A_p = \pi \frac{d^2}{4} = 4in^2. \quad (A-1)$$

Since GLR = 0, fluid is treated as incompressible, the total injection rate is given by

$$q_t = q_g + q_l, \quad (A-2)$$

$$\therefore q_t = 0 + (2bpm \times 5.615 ft^3 / bbl) = 11.23 ft^3 / min.$$

Selecting a time increment ($\Delta t = 1$ sec), the corresponding injected length of mud acid is

$$l_i = \frac{(q_t \times \Delta t)}{A_p} \quad (A-3)$$

$$l_1 = \frac{(11.23 ft^3 / min)(1 min)}{(4in^2)(ft^2 / 144in^2)} = 404 ft$$

Calculate the Reynolds number

$$N_{RE} = \frac{1.48 \rho_l q_t}{\mu_l d}, \quad (A-4)$$

$$N_{RE} = \frac{1.48(67lbm / ft^3)(2bpm)(1440 min / day)}{(1.2cp)(2.259in)} = 105,350$$

Since $N_{RE} > 2100$, this implies turbulent flow and the resulting friction factor is obtained from Chen's³⁹ equation

$$f_{ip} = \left\{ -4 \log \left[\frac{\varepsilon}{3.7065} - \frac{5.0452}{N_{RE}} \log \left(\frac{\varepsilon^{1.1098}}{2.8257} + \left(\frac{7.149}{N_{RE}} \right)^{0.8981} \right) \right] \right\}^{-2}, \quad (A-5)$$

$$f = \left\{ -4 \log \left[\frac{0.0006}{3.7065} - \frac{5.0452}{105350} \log \left(\frac{0.0006^{1.1098}}{2.8257} + \left(\frac{7.149}{105350} \right)^{0.8981} \right) \right] \right\}^{-2} = 5.26 * 10^{-3}$$

The pressure at the bottom of the injected mud acid is then obtained from Eq. 3.41 as $p_2 = 2540 \text{ psi}$. The remaining portion of the wellbore is filled with brine with a corresponding length equal to:

$$l_{Brine} = L - l_1 = (5000 - 404) \text{ ft} = 4,596 \text{ ft}.$$

Setting $p_1 = p_2 = 2540 \text{ psi}$, the calculations are repeated using the same injection rate and the density of Brine. Thus, from Eq. A-4, A-5, and 3.41, the bottomhole pressure obtained is $p_{bh} = 4,034 \text{ psi}$. This value is outputted and the corresponding fluid at the perforation is Brine.

For the next time increment, the injected length of mud acid becomes $l_1 = 807 \text{ ft}$, and the corresponding length of brine is $l_{Brine} = 4,193 \text{ ft}$. The calculations outlined above are repeated and the corresponding bottomhole pressure obtained. This is continued until all the mud acid has been injected (i.e. $\Delta t = 3 \text{ sec}$).

The next injected fluid is Foam. From the linear temperature distribution assumption along the wellbore length, the temperature at any portion of the wellbore is calculated from

$$T = T_{surf} + \frac{(T_{bh} - T_{surf})}{L} l \sin \theta . \quad (\text{A-6})$$

The in-situ gas flowrate in ft^3/min is obtained from

$$q_g = 0.0283 \times (q_l \times GLR) \frac{T}{p}, \quad (\text{A-7})$$

$$q_g = 0.0283 \times (1bpm)(1,800scf / bbl) \frac{(82.4 + 460)^{\circ} R}{(2400 + 14.7)psia} = 11.5 \text{ ft}^3 / \text{min} .$$

The total injection rate from Eq. A-2 is

$$q_t = 17.2 \text{ ft}^3 / \text{min} .$$

With the same time increment, the corresponding injected length from Eq. A-3 is $l_2 = 619 \text{ ft}$. Due to the compressible nature of foam, an iterative procedure has to be carried out; therefore a foam length segment and corresponding pressure drop in that segment has to be assumed:

$$\Delta l_2 = 2.5 \text{ ft} ,$$

and

$$(\Delta p)_{assumed} = 1\%(p_1) = 0.01 \times 2400 = 24 \text{ psi} .$$

The corresponding average segment pressure given by

$$p_{av} = p_1 + \frac{(\Delta p)_{assumed}}{2}, \quad (\text{A-8})$$

$$p_{av} = 2412 \text{ psi} .$$

With the procedure outlined in section 3.3 the gas compressibility factor is obtained as $z = 1.01$. The gas Formation Volume Factor (FVF), B_g , is calculated from

$$B_g = 0.0283 \frac{zT_{av}}{P_{av}}, \quad (\text{A-9})$$

$$B_g = 6.42 \times 10^{-3} \text{ ft}^3 / \text{scf} .$$

The corresponding in-situ gas flowrate is

$$q_g = (q_l \times GLR) \times B_g, \quad (\text{A-10})$$

$$q_g = 11.56 \text{ ft}^3 / \text{min} ,$$

and the corresponding in-situ gas volume is

$$V_g = (q_g \times \Delta t) = 11.56 \text{ ft}^3$$

The liquid phase volume is

$$V_l = q_l \times \Delta t = (1 \text{ bpm}) \times (5.615 \text{ ft}^3 / \text{bbl}) \times (1 \text{ min}) = 5.62 \text{ ft}^3$$

From Eq. 2.1, the in-situ quality of foam is $\Gamma = 0.67$. From the procedure outlined in section 3.2.2, the viscosity of foam is calculated as follows:

Calculate the true yield stress. Since $\Gamma > 0.6$,

$$\therefore \tau_{yp} = 0.0002 \times \exp(9\Gamma) = 0.083 \text{ lbf} / \text{ft}^2 .$$

Calculate the temperature-dependent flow behavior index from Eq. 3.11

$$n_T = 1.011 .$$

and the temperature-dependent liquid consistency index from Eq. 3.12 is

$$K_T = 1.77 \times 10^{-5} \text{ lbf} - \text{sec} / \text{ft}^2 .$$

Calculate foams consistency-index exponent are

$$C_1 = 4,$$

and

$$C_2 = 0.0023.$$

The consistency index of foam is obtained from Eq. 3.14

$$K_f = 3.67 \times 10^{-4} \text{ lbf} \cdot \text{sec} / \text{ft}^2.$$

Eq. 2.5 gives the apparent yield stress from HB model as

$$\tau'_{yp} = 0.114 \text{ lbf} / \text{ft}^2.$$

The in-situ gas density is calculated from Eq. 3.2

$$\rho_g = 11.58 \text{ lbm} / \text{ft}^3.$$

Superficial phase velocities are obtained from the respective flowrates

$$v_{sl} = \frac{q_l}{A_p} = 3.36 \text{ ft} / \text{s},$$

and

$$v_{sg} = \frac{q_g}{A_p} = 6.92 \text{ ft} / \text{s}.$$

The corresponding in-situ foam velocity is

$$v_f = 10.28 \text{ ft} / \text{s}.$$

The mass flowrates are obtained from

$$\begin{aligned} \dot{m}_l &= q_l \times \rho_l = (1 \text{ bpm}) \times (5.615 \text{ ft}^3 / \text{bbl}) \times (1 \text{ min} / 60 \text{ sec}) \\ &\quad \times (60 \text{ lbm} / \text{ft}^3) = 5.615 \text{ lbm} / \text{s}, \end{aligned}$$

and

$$\dot{m}_g = q_g \times \rho_g = (11.56 \text{ ft}^3 / \text{min}) \times (1 \text{ min} / 60 \text{ sec}) \times (11.58 \text{ lbm} / \text{ft}^3) = 2.23 \text{ lbm} / \text{s} .$$

From Eq. 3.16, the apparent viscosity of foam is obtained as $\mu_a = 31.6 \text{ cp}$. From Eq. 3.5, the no-slip liquid hold is $\lambda_l = 0.33$. Thus corresponding foam density is:

$$\rho_f = \rho_l \lambda_l + \rho_g (1 - \lambda_l) = 60(0.33) + 11.58(1 - 0.33) = 27.4 \text{ lbm} / \text{ft}^3 .$$

Now to establish the flow regime (laminar or turbulent), both frictional pressure drop across the pipe segment for both regimes will have to be calculated and the largest value determines the regime. For laminar flow, the Reynolds number in field units is given by

$$(N_{RE})_f = \frac{1.48 \rho_f q_t}{\mu_l D} , \quad (\text{A-11})$$

$$(N_{RE})_f = 1,993 .$$

And the Fanning friction factor is obtained from Eq. 3.19 $f_f = 8.03 \times 10^{-3}$. The frictional pressure drop is obtained from Eq. 3.23 as

$$(\Delta p_f)_{Laminar} = 7.68 \text{ psi} .$$

For turbulent flow, the scale-up method described in section 3.2.2 is used to obtain the turbulent friction factor as

$$f_f = 6.37 \times 10^{-3} ,$$

and the corresponding pressure drop is

$$(\Delta p_f)_{Turbulent} = 7.7 \text{ psi} .$$

Comparing both calculated pressure drops, it is evident that turbulent flow is dominant (larger Δp_f value); therefore its friction factor would be used in the mechanical energy solution in Eq. 3.32. The constants obtained from integrating Eq. 3.31 are calculated and Eq. 3.32 is solved iteratively to get the pressure at the bottom of the segment as $p_2 = 2,401 \text{ psi}$; which is a pressure drop of 1 psi .

This is a lot smaller than what was assumed initially; therefore updating the assumed pressure drop across the segment, $(\Delta p)_{assumed} = 1 \text{ psi}$, the corresponding average pressure across the segment becomes $p_{av} = 2400.5 \text{ psi}$. The entire calculations are repeated. The new pressure obtained is $p_2 = 2,402 \text{ psi}$, which corresponds to a pressure drop of 2 psi . This is close enough to the assumed value of 1 psi ; therefore the iteration for that segment is stopped.

This becomes the new surface pressure for the next segment length of foam, and the whole process is repeated until all the segments add up to the length of the injected foam length. The pressure at the bottom of the foam injected length then becomes $p_2 = 2,423 \text{ psi}$, which is also the pressure at the top of the previously injected mud acid column. With this new pressure, the pressure-drop calculations are performed again but with a flowrate of 3bpm (total injection rate of foam). The pressure at the bottom of the mud acid column obtained using the calculations outlined before is $p_2 = 2,791 \text{ psi}$.

The remaining portion of the wellbore is filled with brine with a corresponding length equal to $l_{Brine} = L - (l_1 + l_2) = (5000 - (404 + 619)) \text{ ft} = 3,977 \text{ ft}$.

Setting the pressure at the top of the brine fluid column to $2,791\text{ psi}$, the calculations are repeated using the same injection rate and the density of Brine. Thus, from Eq. A-4, A-5, and 3.41, the bottomhole pressure obtained is $p_{bh} = 3,691\text{ psi}$. This value is outputted and the corresponding fluid at the perforation is Brine. For the next time increment, the injected length of foam becomes, and the calculations are repeated again until all the foam has been injected (i.e. $\Delta t = 4\text{ sec}$).

The last fluid involves the filling of the entire wellbore with Brine. Starting with a time increment, the corresponding length of Brine is $l_3 = 403\text{ ft}$. With the new surface pressure and injection rate, the pressure at the bottom of the Brine column is $2,531\text{ psi}$. This then becomes the pressure at the top of the previously injected foam column.

Assuming a pressure drop across the entire foam column of 93 psi based on the previous calculations, the average pressure becomes 2577 psi . Using this average pressure, the PVT properties are calculated and the new corresponding foam column length becomes $l'_2 = 2,420\text{ ft}$. With this new length, the iterative process is carried out to give the pressure at the bottom of the foam column as $2,574\text{ psi}$; which translates to a pressure drop of 44 psi . This is significantly different from what was assumed (93 psi). Thus, updating the assumed pressure drop value, the process is repeated to obtain a new foam column length of $2,435\text{ ft}$ and a corresponding pressure of $2,574\text{ psi}$ at the bottom of the foam column.

This becomes the pressure at the top of the mud acid injected previously, and the pressure drop calculations are carried out as before. The entire process is repeated until

the last injected fluid (Brine) as displaced all the fluids into the formation and filled up the entire wellbore.

Table A-3 below shows the result of the entire calculation along with the fluid position both at the surface and perforation.

Time, min	Surface pressure, psi	BHP, psi	Q, bpm	Fluid at surface	Fluid at perf
1	2400	4035	2	Mud acid	Brine
2	2400	4044	2	Mud acid	Brine
3	2400	4054	2	Mud acid	Brine
4	2400	3691	1	Foam	Brine
5	2400	3538	1	Foam	Brine
6	2400	3382	1	Foam	Brine
7	2400	3229	1	Foam	Brine
8	2400	3306	2	Brine	Brine
9	2400	3365	2	Brine	Brine
10	2400	3424	2	Brine	Brine
11	2400	3484	2	Brine	Brine
12	2400	3543	2	Brine	Mud acid
13	2400	3608	2	Brine	Mud acid
14	2400	3681	2	Brine	Mud acid
15	2400	3761	2	Brine	Mud acid
16	2400	3850	2	Brine	Mud acid
17	2400	3926	2	Brine	Foam
18	2400	3978	2	Brine	Foam
19	2400	4000	2	Brine	Foam
20	2400	4025	2	Brine	Brine

VITA

Name: Efejera A. Ejofodomi

Permanent Address: 8B Akin Osiyemi Street, Off Allen-Avenue
Ikeja, Lagos. Nigeria.

Email Address: efejera@yahoo.com

Education: M.S Petroleum Engineering
Texas A&M University
College Station, USA, 2006.

B.S. Mechanical Engineering
University of Lagos (UNILAG)
Lagos, Nigeria, 2002.